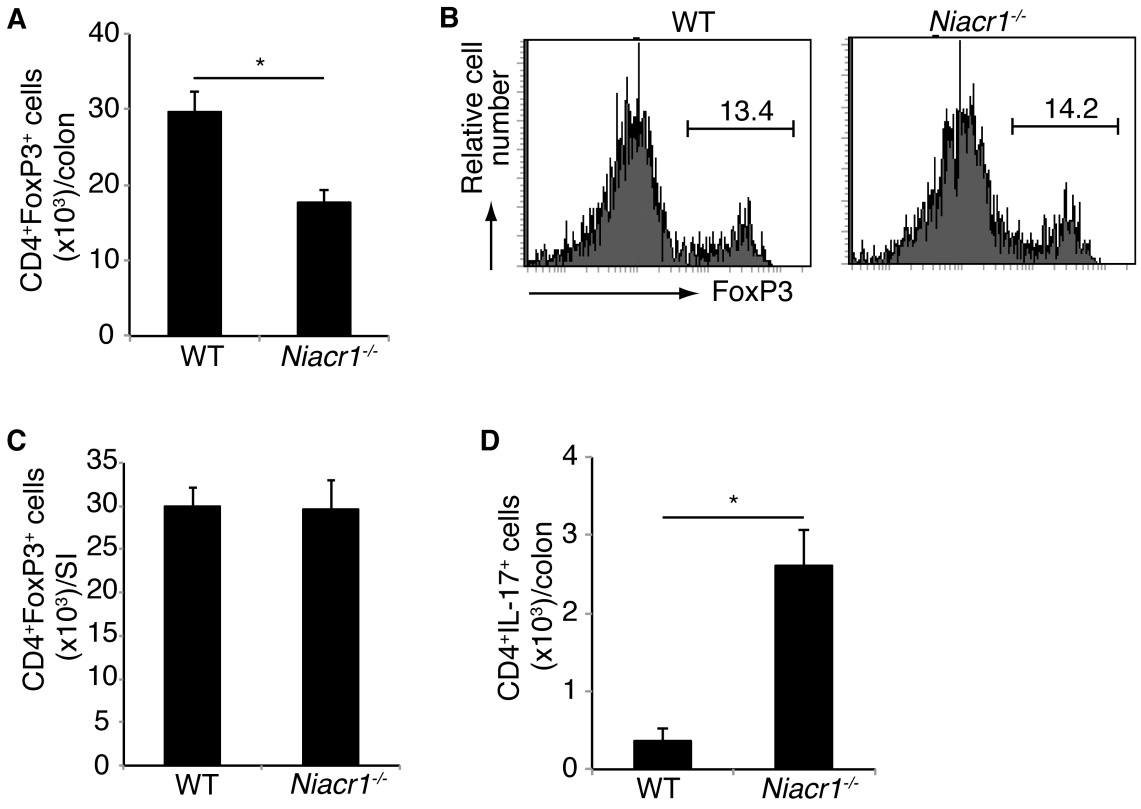

Figure S1. Reduced Treg ($CD4^+FoxP3^+$) and increased Th17 ($CD4^+IL\text{-}17^+$) cells in colons of *Niacr1*$^{-/-}$ mice. Related to Figure 1.

(A) Number of $CD4^+FoxP3^+$ T cells in colons of WT and *Niacr1*$^{-/-}$ mice (n=3). *P<0.003

(B) FoxP3 expression by $CD4^+$ T cells from small intestines of WT and *Niacr1*$^{-/-}$ mice.

(C) Number of $CD4^+FoxP3^+$ T cells in small intestines of WT and *Niacr1*$^{-/-}$ mice (n=3).

(D) Number of $CD4^+IL\text{-}17^+$ T cells in colons of WT and *Niacr1*$^{-/-}$ mice (n=3). *P<0.002

A representative of 3 experiments is shown.

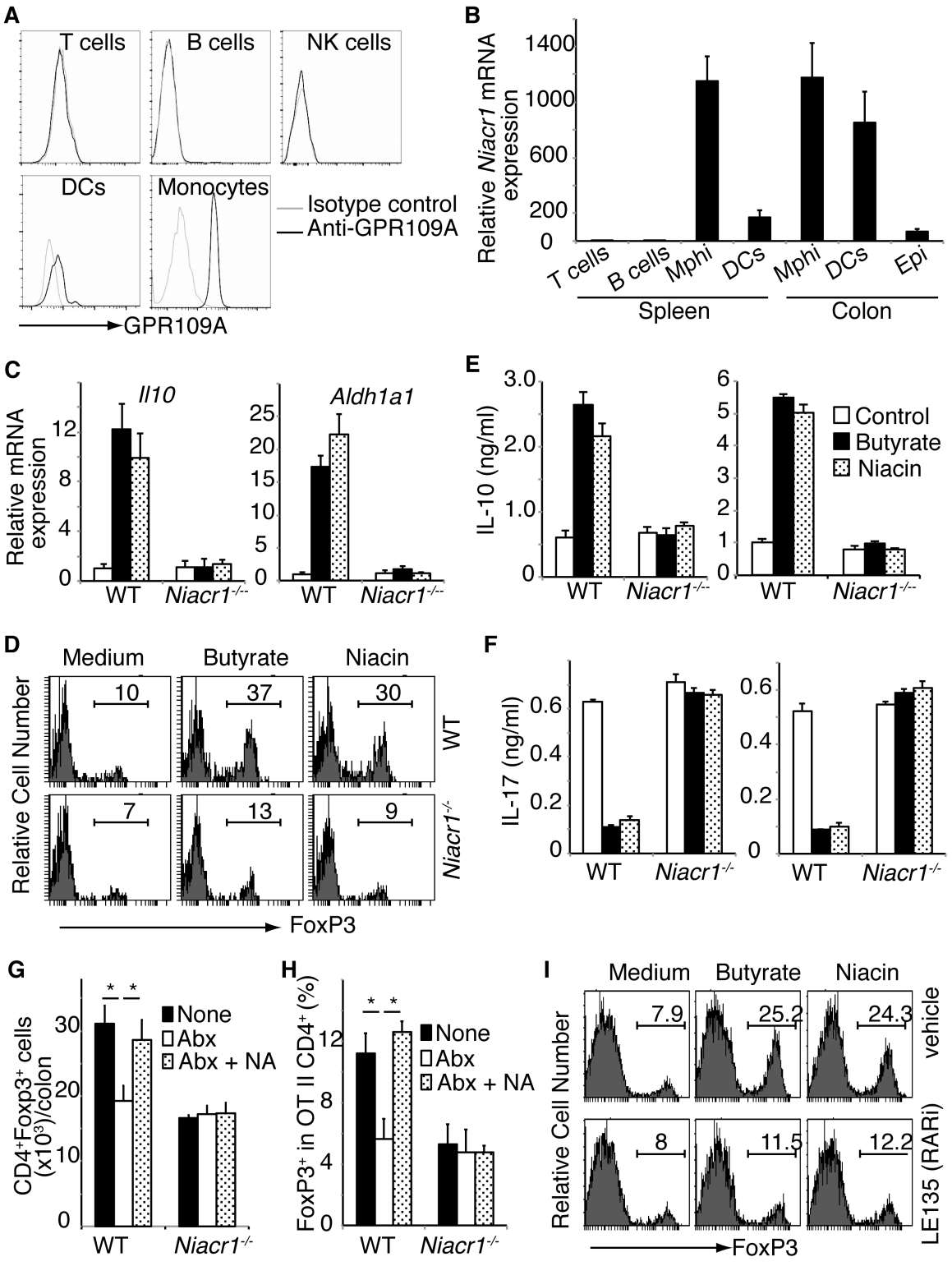

Figure S2. Butyrate and niacin induce an anti-inflammatory phenotype in DCs and macrophages through Gpr109a. Related to Figure 2.

(A) Human peripheral blood mononuclear cells (PBMCs) were stained with antibody against GPR109A or isotype control antibody. Shown are the staining levels of GPR109A compared to those obtained with isotype control antibody. T cells, B cells and NK cells were identified as $CD3^+$, $CD3^-$ and $CD56^+$ populations, respectively, in lymphocyte gating. $CD123^+$ cells were classified as dendritic cells, and $CD14^+$ cells as monocytes.

(B) Single-cell suspension from spleen of WT mice was sorted into populations of T cells ($CD90^+$), B cells ($CD19^+$), DCs ($CD11c^+$) and macrophages ($CD11b^+$). Similarly, DCs ($CD45^+I\text{-}A^{b+}CD11b^+$) and macrophages ($CD45^+I\text{-}A^{b+}CD11b^+$) and epithelium were isolated from colons of WT mice. Expression of *Gpr109a* was quantified using qPCR. Values represent mean ± standard deviation of triplicates.

(C) Splenic macrophages ($CD11b^+$ cells) from indicated mice were cultured in the presence or absence of butyrate or niacin. Two-days later, expression levels of *Il10* and *Aldh1a1* were quantified by qPCR. Values represent mean ± standard deviation of triplicates.

(D) Splenic macrophages were treated with butyrate or niacin as above and used as APCs in differentiation assay for OT-II $CD4^+$ T cells as in Figure 2E. Four days later, cells were stained for CD4 and FoxP3. Histograms show FoxP3 expression by $CD4^+$ T cells.

(E-F) Naïve OT-II $CD4^+$ T cells were differentiated with butyrate- or niacin-treated splenic $CD11c^+$ or $CD11b^+$ cells from WT and *Niacr1*$^{-/-}$ mice. Differentiated $CD4^+$ T cells were re-stimulated overnight, and IL-10 and IL-17 in culture supernatants was measured by ELISA.

(G) Number of $CD4^+FoxP3^+$ in colons of mice from Figure 2F. *$P<0.01$

(H) WT or *Niacr1*$^{-/-}$ (both $Thy1.2^+$) were treated with antibiotics in the presence or absence of niacin in drinking water for 3 weeks. Subsequently, mice received OTII T cell (Thy1.1+) intravenously and ovalbumin in drinking water. One week later FoxP3 expression by OTII $CD4^+$ T cells ($Thy1.1^+CD4^+$) in the colons of mice was analyzed. *$P<0.007$

(I) Splenic DCs from WT mice were treated with butyrate or niacin and used as APCs in differentiation assays for OT-II $CD4^+$ T cells. T cell differentiation was carried out in the presence or absence of RAR inhibitor (RARi) LE135 (1 μM). Shown is the Foxp3 expression by $CD4^+$ T cells.
A representative of at least 2 experiments is shown.

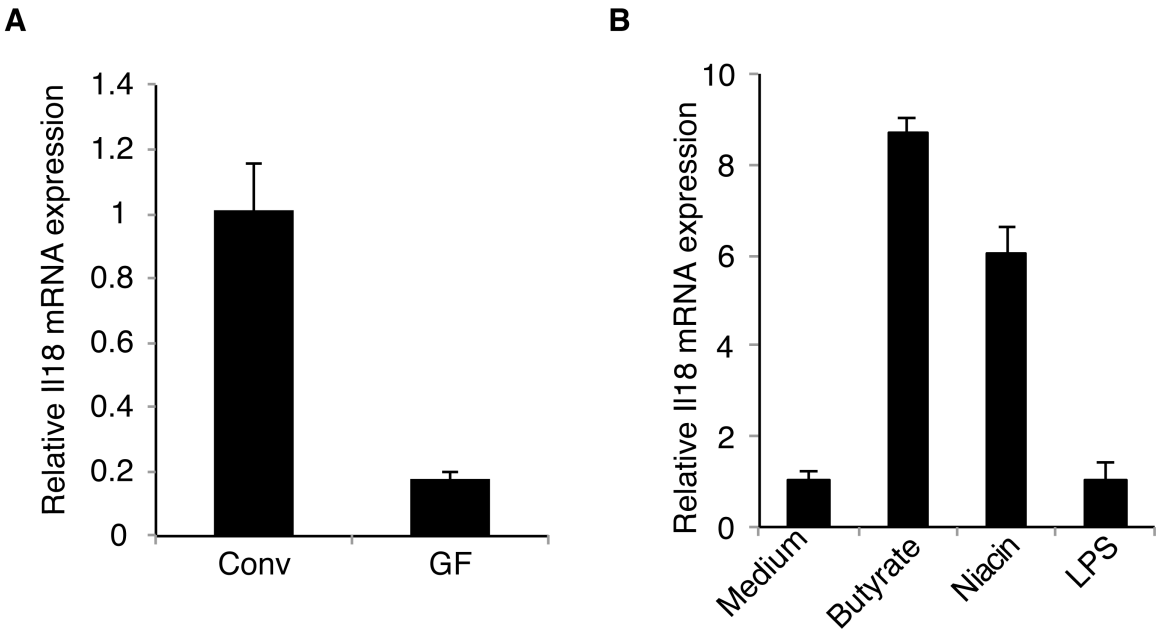

Figure S3. Commensal metabolite butyrate and niacin induces *Il18* mRNA in colon. Related to Figure 3.

(A) Expression of *Il18* mRNA in colons of germ-free (GF) and conventionally raised mice (n=4 mice/group)

(B) Colons of neonatal WT mice were cultured in the presence of butyrate, niacin or LPS for 24 h, and *Il18* mRNA was quantified by qPCR. Values represent mean ± standard deviation of triplicates.

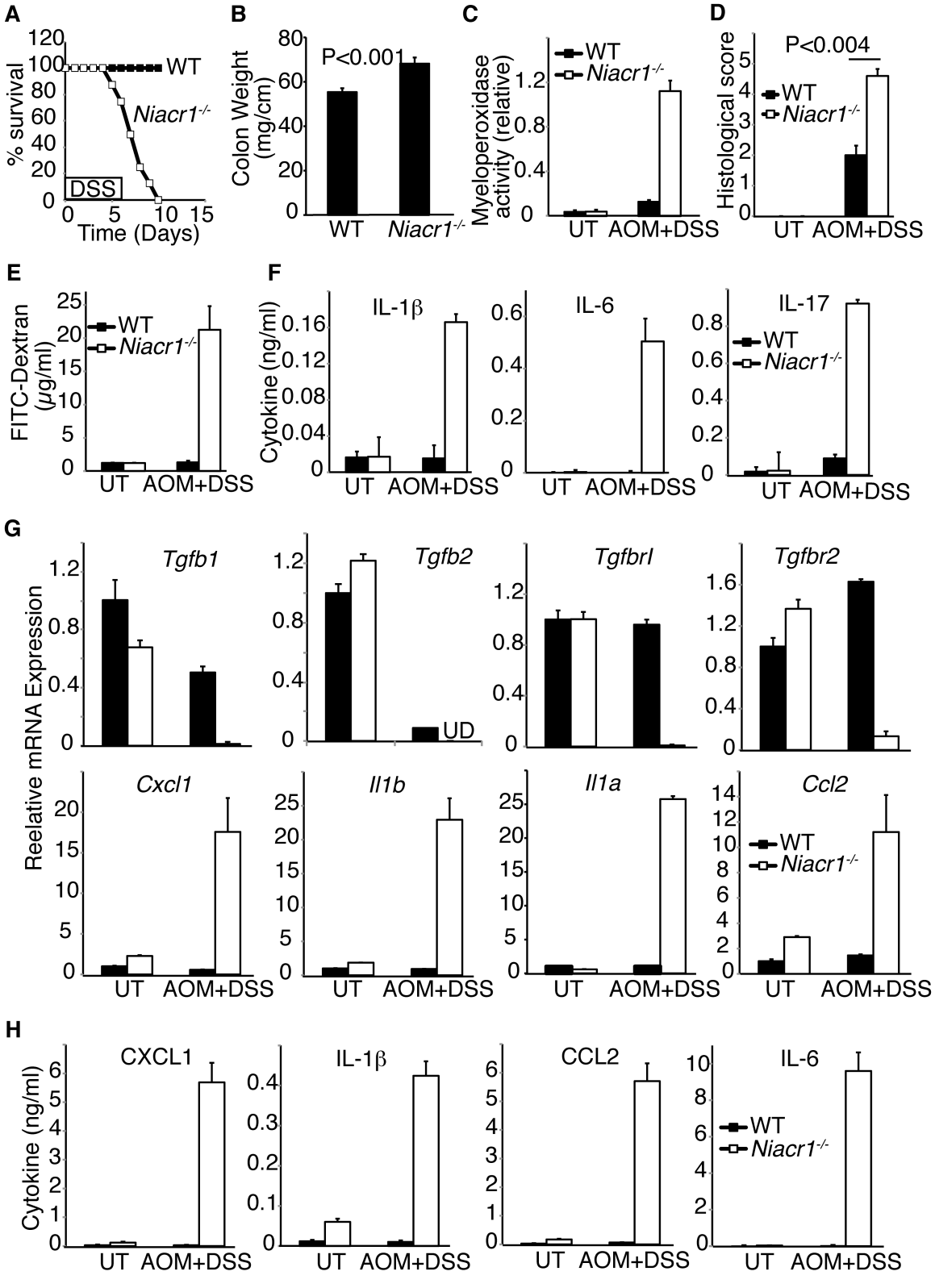
A
% survival
WT
Niacr1-/-
DSS
Time (Days)
B
Colon Weight (mg/cm)
P<0.001
WT
Niacr1-/-
C
Myeloperoxidase activity (relative)
WT
Niacr1-/-
UT AOM+DSS
D
Histological score
P<0.004
WT
Niacr1-/-
UT AOM+DSS
E
FITC-Dextran (μg/ml)
WT
Niacr1-/-
UT AOM+DSS
F
IL-1β
IL-6
IL-17
Cytokine (ng/ml)
WT
Niacr1-/-
UT AOM+DSS
G
Reelative mRNA Expression
Tgfb1
Tgfb2
UD
Tgfbrl
Tgfbr2
Cxcl1
Il1b
Il1a
Ccl2
WT
Niacr1-/-
UT AOM+DSS
H
Cytokine (ng/ml)
CXCL1
IL-1β
CCL2
IL-6
WT
Niacr1-/-
UT AOM+DSS

Figure S4. Hypersusceptibility of *Niacr1*$^{-/-}$ mice to colonic inflammation and epithelial barrier disruption. Related to Figure 4

(A) WT and *Niacr1*$^{-/-}$ mice were fed with 3% DSS in drinking water for 6 days and their survival was monitored. The data are given as a Kaplan-Meier plot (n=8 mice).
(B-H) Mice of indicated genotypes were treated as shown in Figure 4A. On 20th day of AOM+DSS regime, mice were analyzed for indicated parameters.
(B) Colon weight/cm length (n=4).
(C) Myeloperoxidase activity in colon (n=5).
(D) Histopathological score (inflammation + epithelial damage) of colons was graded following analysis of H&E stained cross section of colons of untreated (UT) or (AOM+DSS)-treated of indicated genotypes.
(E) Mice were fed with FITC-dextran, and 4 h later FITC-dextran was quantified in serum (n=5).
(F) Inflammatory cytokines in sera of mice were quantified by ELISA (n=5).
(G) RNA was extracted from colons of untreated and (AOM +DSS)-treated WT and *Niacr1*$^{-/-}$ mice. Expression of indicated genes was quantified by qPCR. UT, untreated, UD, undetectable.
(H) Colons of AOM+DSS treated mice of indicated genotypes were harvested and organ cultures were setup. Culture supernatants were harvested 24 h later. Cytokines in culture supernatants were measured by ELISA (n=5). UT; untreated.

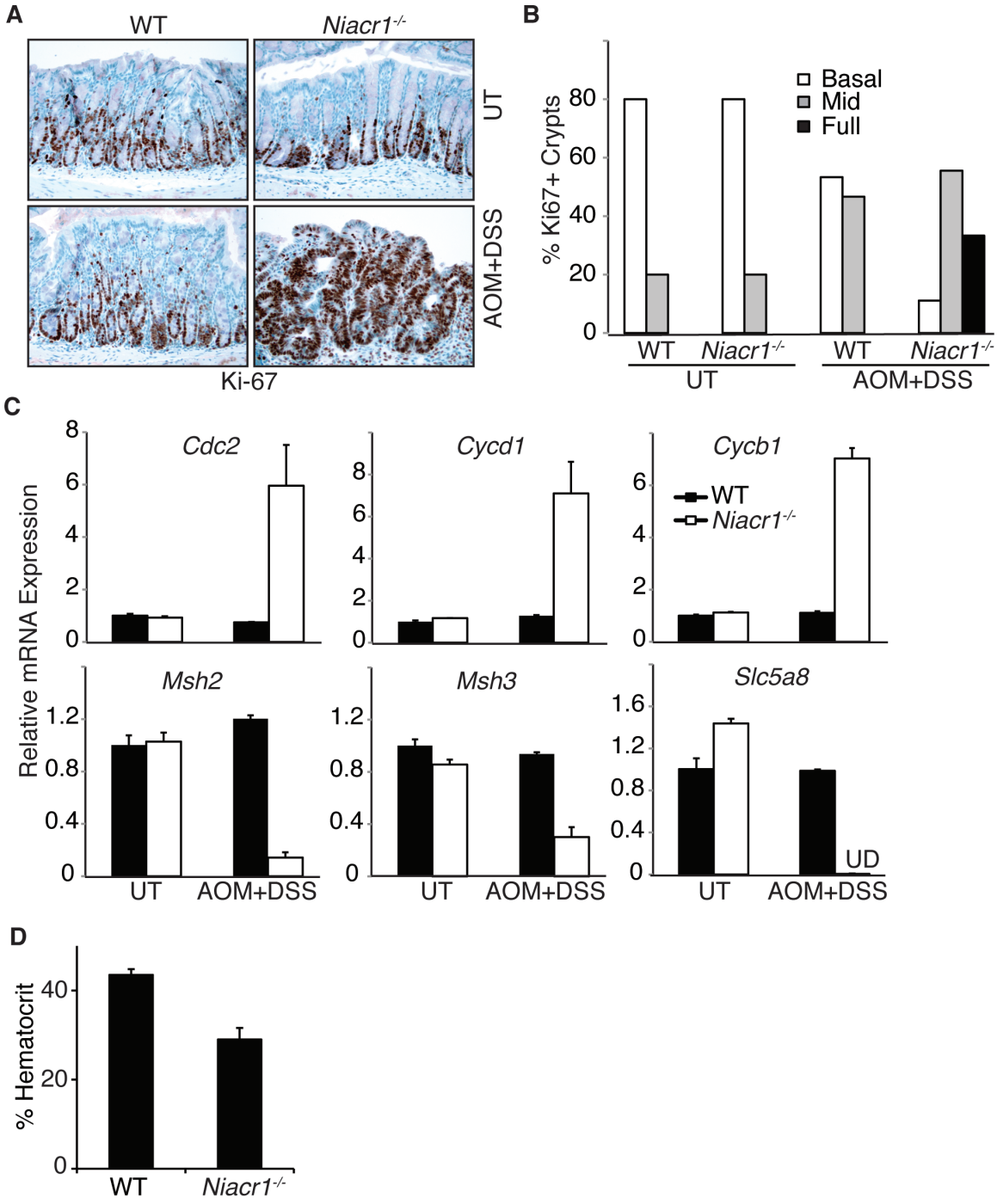

Figure S5. Enhanced colon carcinogenesis in (AOM+DSS)-treated *Niacr1*$^{-/-}$ mice. Related to Figure 5.

(A) Representative images of Ki-67 staining in colonic sections from untreated or day 20 of AOM+DSS regime. Brown and blue color represent staining for Ki-67 and nucleus respectively.

(B) Distribution of size of epithelial cell proliferative compartments in crypts of colons. Data was calculated after analysis of Ki67 staining (as in A) of colonic cross sections (n=3).
(C) Relative expression of cell cycle promoters (*Cdc2*, *Cycd1*, *Cycb1*), DNA mismatch repair genes (*Msh2*, *Msh3*) and tumor suppressor *Slc5a8* in colons of (AOM + DSS)-treated mice with indicated genotype. UT; untreated, UD; undetectable (n=3).
(D) At the completion of AOM+DSS treatment, hematocrit was determined in WT and *Niacr1*$^{-/-}$ mice (n=4).

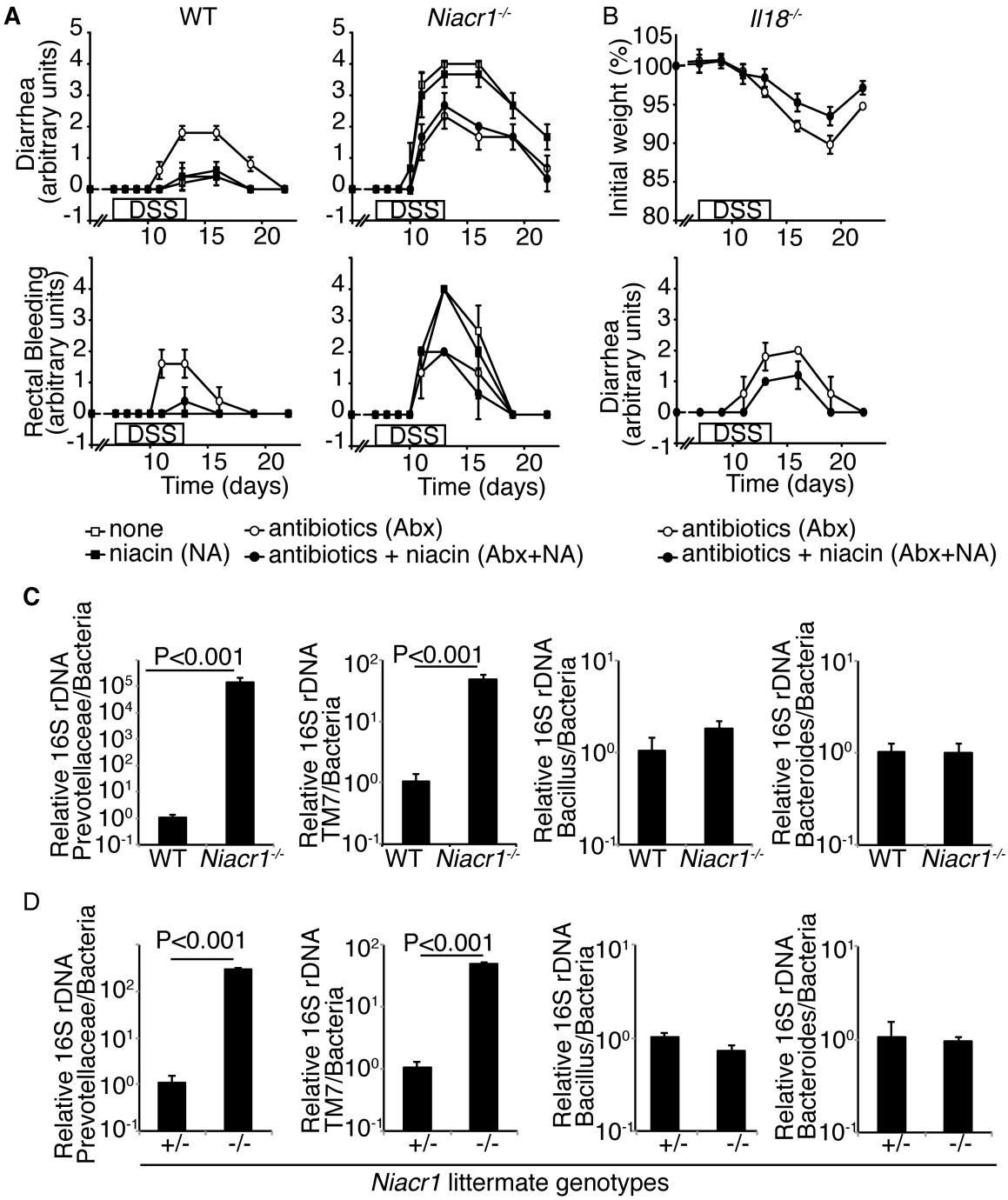

Figure S6 Role of Gpr109a and IL-18 in niacin induced suppression of antibiotics induced susceptibility to colonic inflammation. Related to Figure 7.
(A) Diarrhea and rectal bleeding in WT and *Niacr1*$^{-/-}$ treated in Figure 7B (n≥4).
(B) *Il18*$^{-/-}$ mice were treated with antibiotics in the presence or absence of niacin as in Figure 7A. Shown is the weight loss and diarrhea (n= 5 mice)

(C) Quantification of indicated bacterial groups in feces of WT and *Niacr1*$^{-/-}$ mice by qPCR. Amounts of indicated bacteria groups were first normalized to that of total bacteria for each sample. Abundance of each bacterial group in the feces from WT mice was taken as 1 to calculate the relative abundances of corresponding bacterial group in feces from *Niacr1*$^{-/-}$ mice (n=5).
(D) Abundance of *Prevotellaceae, TM7, Bacillus and Bacteroides group of commensals* in the feces of 3-month-old *Niacr1*$^{+/-}$ and *Niacr1*$^{-/-}$ littermates, weaned at 21 days of age was quantified as in (C) (n=3).

Supplementary Table 1. Sequences of PCR primers used in this study

Genes	Primer Sequences
Il1a	Forward, 5'-CGGGTGACAGTATCAGCAAC-3'
	Reverse, 5'-GACAAACTTCTGCCTGACGA-3'
Il1b	Forward, 5'-CCCAACTGGTACATCAGCAC-3'
	Reverse, 5'-TCTGCTCATTCACGAAAAGG-3'
Il6	Forward, 5'-CTACCCCAATTTCCAATGCT-3'
	Reverse, 5'-ACCACAGTGAGGAATGTCCA-3'
Il10	Forward, 5'-AGTGGAGCAGGTGAAGAGTG-3'
	Reverse, 5'-TTCGGAGAGAGGTACAAACG-3'
Il11	Forward, 5'-AACTGTGTTTGTGGCCTGGT-3'
	Reverse, 5'-CGTCAGCTGGGAATTTGTCT-3'
Il17a	Forward, 5'-GCTCCAGAAGGCCCTCAGA -3'
	Reverse, 5'-AGCTTTCCCTCCGCATTGA-3'
Il18	Forward, 5'-CCTCAGATCTTCTGCAACCT-3'
	Reverse, 5'-TTCCGTATTACTGCGGTTGT-3'
Aldh1a1	Forward 5'-CTGTGCAGGCTGGGCTGACAA-3'
	Reverse 5'- AAAATTCCAGGGGATTTGGCCA-3'
bact16s	Forward 5'-AGAGTTTGATCCTGGCTCAG-3'
	Reverse 5'- GGACTACCAGGGTATCTAAT-3'
Ccl2	Forward, 5'-TGCTACTGATTCACCAGCAA-3'
	Reverse, 5'-GTCTGGACCCATTCCTTCTT-3'
Cdc2	Forward, 5'-TCGCATCCCACGTCAAGA-3'
	Reverse, 5'-GTTTGGCAGGATCATAGACTAGCA-3'
CycB1	Forward, 5'-ACTTCAGCCTGGGTCGCC-3'
	Reverse, 5'-ACG TCAACCTCTCCGACTTTAGA-3'
CycD1	Forward, 5'-CCCTGACACCAATCTCCTCAA-3'
	Reverse, 5'-GCATGGATGGCACAATCTCCT-3'
Cxcl1	Forward, 5'-CCAGAGCTTGAAGGTGTTGC-3'
	Reverse, 5'-TCTGAACCAAGGGAGCTTCA-3'
Gpr109a	Forward 5'- ATGGCGAGGCATATCTGTGTAGCA-3'
	Reverse 5'- TCCTGCCTGAGCAGAACAAGATGA-3'
Msh2	Forward, 5'-AGACCCAGGGCGTGATCAAGTACA-3'
	Reverse, 5'-TTGCCGGGAGAAGCCTTAAATGCC-3'
Msh3	Forward, 5'-CAGTTTGTGCCCAACAGTACGAGT-3'
	Reverse, 5'-AGCACCCATCCtTGTGAAAATGCC-3'
Slc5a8	Forward, 5'-TCGAGTTGGCGAAGGGGACCA-3'
	Reverse, 5'-ATGCCTTGGCGGCAGTCACC-3'
Tgfb1	Forward, 5'-CTCCCGTGGCTTCTAGTGC-3'
	Reverse, 5'-GCCTTAGTTTGGACAGGATCTG-3'
Tgfb2	Forward, 5'-CCTGACCGCTCTGAGAATTA-3'
	Reverse, 5'-ATCCTCTTGCGCATAAACTG-3'
Tgfbr1	Forward, 5'-GAAGTAGTGGCCAGCTGTGT-3'
	Reverse, 5'-GCAGAGGGAAGAGTCAAACA-3'
Tgfbr2	Forward, 5'-AGCGGGGAATTTACAACAGAATG-3'

	Reverse, 5’-GAGGAATGACAGCGATGCTA-3’
Gapdh	Forward, 5’-AGGTCGGTGAACGGATTTG -3’
	Reverse, 5’-TGTAGACCATGTAGTTGAGGTCA -3’
Prevotellaceae	Forward, 5’-CCAGCCAAGTAGCGTGCA-3’
	Reverse, 5’-TGGACCTTCCGTATTACC-3’
TM7	Forward, 5’-GCAACTCTTTACGCCCAGT-3’
	Reverse, 5’-GAGAGGATGATCAGCCAG-3’
Bacteria	Forward, 5’-AGAGTTTGATCCTGGCTC-3’
	Reverse, 5’-TGCTGCCTCCCGTAGGAGT-3’
Bacteroides	Forward 5’-GGTTCTGAGAGGAGGTCCC-3’
	Reverse 5’-GCTGCCTCCCGTAGGAGT-3’
Bacillus	Forward 5’-GCGGCGTGCCTAATACATGC-3’
	Reverse 5’-CTTCATCACTCACGCGGCGT-3’